Adsorptive removal of nickel by modified natural adsorbents: optimization, characterization and application

Qingping Yi[a,b], Ruiyi Fan[c], Huiyu Min[d], Qinglin Zhang[d,e], Zhengrong Luo[d,e,]*

[a]College of Bioengineering, Jingchu University of Technology, Jingmen 448000, China, email: jmyiqingping@126.com
[b]Chinese National WEEE Recycling Engineering Research Center, Jingmen 448124, China
[c]Institute of Fruit Tree Research, Guangdong Academy of Agricultural Sciences, Key Laboratory of South Subtropical Fruit Biology and Genetic Resource Utilization (MOA), Guangdong Province Key Laboratory of Tropical and Subtropical Fruit Tree Research, Guangzhou 510640, China, email: fanruiyi@outlook.com
[d]Key Laboratory of Horticultural Plant Biology (MOE), Huazhong Agricultural University, Wuhan 430070, China, Tel./Fax: +86 27 87282677; emails: luozhr@mail.hzau.edu.cn (Z. Luo), 2513884818@qq.com (H. Min), zhangqinglin@mail.hzau.edu.cn (Q. Zhang)
[e]Hubei Collaborative Innovation Center for the Characteristic Resources Exploitation of Dabie Mountains, Huanggang Normal University, Huanggang 438000, China

ABSTRACT

The adsorptive removal of nickel by persimmon tannin-based adsorbents was first evaluated. NaOH modified persimmon powder-formaldehyde resin (NPPFR) showed significantly enhanced adsorption capacity towards Ni(II). The adsorption process was completely achieved equilibrium within 60 min, and the well-fitted pseudo-second-order kinetics data indicated that chemisorption is the main rate-limiting step. The adsorption isotherms followed the Langmuir model, where the maximum adsorption capacity reached 81.6 mg g^{-1} at pH 5.0. The adsorbed Ni(II) ions were desorbed by 0.1 mol L^{-1} HNO$_3$ and the regenerated adsorbent exhibited undiminished sorption efficiency for 4 cycles. The removal of Ni(II) from actual industrial wastewaters in both batch and column experiments was demonstrated to be effective. The adsorption mechanism was proposed to be electrostatic attraction and ion exchange. In addition, competition and replacement during the adsorption process were found in the multiple metal ions systems. The results indicated that NPPFR can serve as a low-cost, eco-friendly and effective alternative for Ni(II) removal in wastewater treatment.

Keywords: Persimmon residues; Nickel; Removal; Sorption; Wastewater treatment

1. Introduction

Nickel(II) is a toxic pollutant that is found in wastewaters from the electroplating, battery manufacturing and recycling, mineral processing and refining industries [1]. Due to its acute neurotoxic and carcinogenic effects, excessive levels of Ni(II) in waters pose a threat to human beings, causing headaches, dizziness, nausea, coughing, chest pain, dermatitis and chronic asthma [2,3]. According to the WHO guidelines, the maximum permissible concentration of Ni(II) in drinking water is 0.01 mg L^{-1}. For industrial wastewaters, the tolerance limit of Ni(II) is 1.0 mg L^{-1}. However, effluents from industrial processes always contain higher concentrations of nickel than the acceptable limit. Hence the removal of Ni(II) from aqueous solutions is highly essential.

* Corresponding author.

Conventional technologies, such as precipitation, ion exchange, membrane filtration, electroplating, adsorption, etc., have been developed to remove heavy metal ions from various aqueous solutions [2,4]. However, some treatment methods are restricted by either low efficiency or high technical and economic requirements. In recent years, biosorption has emerged as a promising method due to such advantages as high efficiency even at low metal concentrations, easy operation and environmental friendliness [5]. Accordingly, adsorbents prepared from agricultural waste and by-products have been widely studied for metal removal from water, including cashew nutshell [1], orange peel [4], rice bran [6], sugarcane bagasse pith [7], *Moringa oleifera* bark [8], pine bark [9], *Lithothamnium calcareum* algae [10], modified chitosan [11–13], etc.

China is the origin and main producing country of persimmon (*Diospyros kaki* Thunb.). Many persimmon residues such as physiological dropped fruits, artificial thinned fruits, and fruit peels can be employed to produce persimmon powder containing large quantities of tannin, which contains multiple adjacent hydroxyl groups in the form of catechol and pyrogallol. Due to its high affinity towards metal ions, a great number of research works are concerned with persimmon tannin [14–16]. However, the removal of Ni(II) from aqueous solutions by tannin-based adsorbent has rarely been reported. Since persimmon tannin is partly water-soluble, concentrated sulfuric acid and formaldehyde have been used as effective crosslinking agents for immobilization. Additionally, NaOH pretreatment can potentially modify the surface morphology and enhance the binding capacity of bio-adsorbents [6,17]. Here the adsorption behavior towards Ni(II) using modified adsorbent prepared from persimmon residues was investigated. The effects of the initial pH, contact time, Ni(II) initial concentration, temperature, and coexisting metal ions on the removal of Ni(II) from aqueous solutions were investigated in detail. The applicability for Ni(II) removal from actual industrial wastewaters was also studied.

2. Materials and methods

2.1. Chemicals

Ni(NO$_3$)$_2$·6H$_2$O, Pb(NO$_3$)$_2$, Mg(NO$_3$)$_2$·6H$_2$O, Mn(NO$_3$)$_2$·4H$_2$O, Zn(NO$_3$)$_2$·6H$_2$O, NaNO$_3$, KNO$_3$, NaOH, and HNO$_3$ were purchased from Sinopharm Chemical Reagent Co. Ltd., Beijing, China. Stock solution containing 1,000 mg L^{-1} Ni(II) was prepared with deionized water and diluted to a certain concentration. The pH of the solution was adjusted using 0.1 mol L^{-1} HNO$_3$ and/or 0.1 mol L^{-1} NaOH. Deionized water was used throughout the study. All the chemicals applied in the present study were of analytical reagent grade and utilized without any purification. All the solutions were prepared with deionized distilled water.

2.2. Preparation of adsorbents

Tannin-enriched persimmon powder was extracted from astringent persimmon dropped fruits, which were kindly donated by Huikun Agriculture Product Co. Ltd., Gongcheng, China. Four types of persimmon tannin based adsorbents were prepared as follows. Persimmon powder-formaldehyde resin (PPFR) and sulfuric acid cross-linked persimmon powder (SPP) was obtained by immobilizing persimmon powder with formaldehyde and concentrated sulfuric acid, respectively, according to the previously reported methods [18,19]. The adsorbents (10 g) were mixed with 500 mL and 0.25 mol L^{-1} NaOH solutions and stirred for 2 h at room temperature, and then washed with deionized water repeatedly until the pH was neutral. Finally, the adsorbents were dried in an oven at 343 K. The alkali-treated adsorbents prepared by modifying PPFR and SPP were named NaOH modified persimmon powder-formaldehyde resin (NPPFR) and NSPP, respectively.

2.3. Adsorption experiments

Adsorption tests of Ni(II) were carried out in batch mode. Typically, 20 mg dry adsorbent was mixed with 20 mL working solution and shaken in a thermostatic shaking incubator (Thermo Scientific MaxQ 4000) at a speed of 200 rpm. Then, the mixture was filtered and the metal ion concentration in the filtrate was measured. The percent adsorption (%Adsorption) and the amount of Ni(II) (*q*) adsorbed onto the adsorbent were calculated according to Eqs. (1) and (2), respectively.

$$\%\text{Adsorption} = \frac{C_i - C_e}{C_i} \times 100 \qquad (1)$$

$$q = \frac{C_i - C_e}{W} \times V \qquad (2)$$

where C_i (mg L^{-1}) and C_e (mg L^{-1}) are the initial and equilibrium concentration of metal ions in solution, respectively. W (mg) is the weight of adsorbent and V (mL) is the volume of the test solution.

To examine the effect of pH, the Ni(II)-solution was adjusted to pH 2.0–7.0. The adsorption isotherm was studied at 303 K with different initial Ni(II) concentrations (20–200 mg L^{-1}). For the kinetics study, 60, 80, and 100 mg L^{-1} of Ni(II) solutions were reacted with NPPFR for various time (5–120 min). The effect of coexisting metal ions on Ni(II) was investigated in binary systems of Ni(II) and Pb(I), Zn(II), Mn(II), Mg(II), K(I) and Na(I).

Regarding the applicability of Ni(II) removal from actual industrial wastewaters, the effect of adsorbent dose was investigated and column adsorption-elution studies were performed. First, 500 mg NPPFR, which was immersed in deionized water for 12 h before use, was packed into a glass column (1 cm × 30 cm). Then, a feed solution consisting of an industrial sample was percolated through a glass column equipped with a constant flow pump (Shanghai Huxi DHL-A) at a constant flow rate of 0.15 mL min^{-1}. The effluent solutions were collected at 60 min intervals by automatic fraction collection (Shanghai Huxi BSA-100) for measuring the metal ion concentration. Once the column reached adsorption saturation, the packed adsorbent was first washed with deionized water for 12 h. Then, the loaded metal ions were eluted with 0.1 mol L^{-1} HNO$_3$. The eluted solution was also collected and analyzed. Under the experimental conditions,

the wet volume of NPPFR was 0.9 mL. The bed volume (B.V.) of the effluent was defined according to Eq. (3).

$$B.V. = \frac{v \times t}{V} \qquad (3)$$

where v, t and V are the flow rate of the solution (0.15 mL min^{-1}), the time (min) for which the feed solution was pumped through the column bed, and the wet volume of the packed adsorbent, respectively.

2.4. Instrumentation

The metal ion concentrations of the samples were measured by an atomic absorption spectrophotometer (AAS, Varian Spectra AA 220). Fourier transform infrared (FT-IR) spectra were recorded by a Nicolet 6700 spectrophotometer using the KBr pellet method. Scanning electron microscopy (SEM) coupled with energy-dispersive X-ray spectroscopy (EDS) facility was performed using a Hitachi SU8010 field emission scanning electron microscopy. The Brunauer–Emmett–Teller surface area and pore volume of the raw materials and modified adsorbents were determined by a surface area analyzer (NOVA 4000e, Quantachrome Instrument, USA).

3. Results and discussion

3.1. Effects of modification methods and solution pH

Common chemical pretreatments can be performed with acids, alkalis and organic solvents, and these treatment methods have been preferred due to their simplicity and efficiency [6,20]. Here the effect of different chemical modifications of persimmon powder (PPFR, SPP, NPPFR and NSPP) on Ni(II) removal was investigated, and the adsorption capacities of these adsorbents towards Ni(II) at different pH values ranging from 2.0–7.0 are shown in Fig. 1. Treatment with sulfuric acid may destroy the hydroxyl groups of the
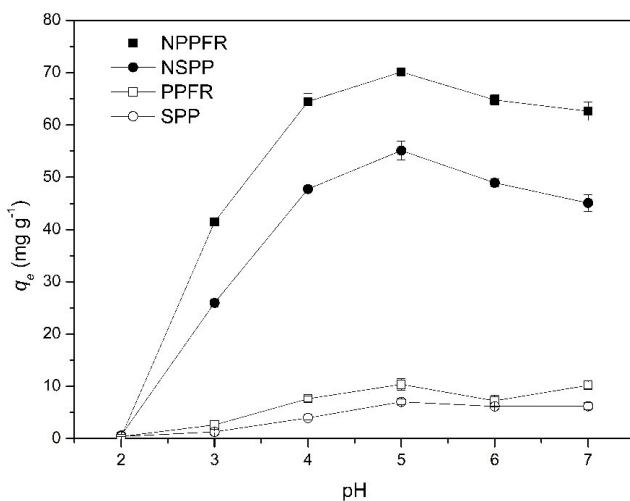
adsorbent, thus the adsorption capacity of Ni(II) by SPP was reduced compared with that of PPFR. The NaOH-modified adsorbents NPPFR and NSPP showed enhanced biosorption capacities compared with the native adsorbents PPFR and SPP. Due to the chemical structure-property of adjacent polyhydroxyphenyl groups, some phenolic hydroxyl can react with NaOH leading to hydrogen replacement by sodium. The texture parameters of PPFR and NPPFR were investigated by the N$_2$ adsorption–desorption technique. The surface area, pore size and pore volume are presented in Fig. 2. It was shown that NPPFR had an enhanced surface area after modification. The significant improvement in sorption capacity may be caused by the exposure of more metal binding sites and the stronger affinity between sodium and Ni(II). The adsorption of Ni(II) is strongly dependent on the initial pH of the aqueous solution.

At low pH, cationic ions Ni(II) and protons compete for vacant sites on the adsorbent resulting in low adsorption of Ni(II). When the pH increased, the adsorbent surface was more negatively charged and the adsorption of Ni(II) increased sharply, and then decreased slightly. At pH values higher than 7.0, precipitation of Ni(II) ions such as Ni(OH)$_2$ occurs simultaneously and might lead to an inaccurate interpretation of adsorption properties [6,7]. The maximum adsorption capacity of NPPFR was observed at pH 5.0. Hence, the rest of the Ni(II) adsorption experiments were carried out by using NPPFR at pH 5.0.

3.2. Effect of contact time and kinetics

The adsorption kinetics of Ni(II) onto the preferred adsorbent NPPFR under varied contact times (5–120 min) and for initial concentrations of 60, 80, and 100 mg L^{-1} are illustrated in Fig. 3. The amount of Ni(II) adsorbed onto the adsorbent increased sharply in the initial 20 min and reached equilibrium at approximately 60 min for all the experimental initial concentrations. The adsorption kinetic of NPPFR was fast while its specific surface area was very small, indicating that the adsorption of Ni(II) should take

Fig. 1. Effects of modification methods and pH on the adsorption of Ni(II). Adsorbent dosage = 1 g L^{-1}, C_i = 80 mg L^{-1}, 303 K.
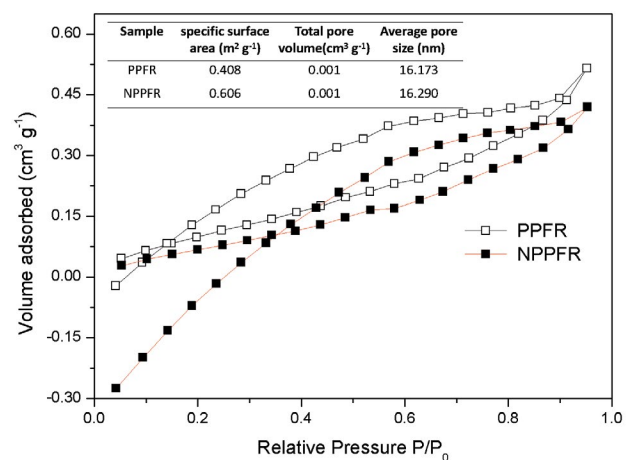
Fig. 2. N$_2$ adsorption–desorption isotherm of PPFR and NPPFR (inset: the surface area, pore size and pore volume of PPFR and NPPFR).
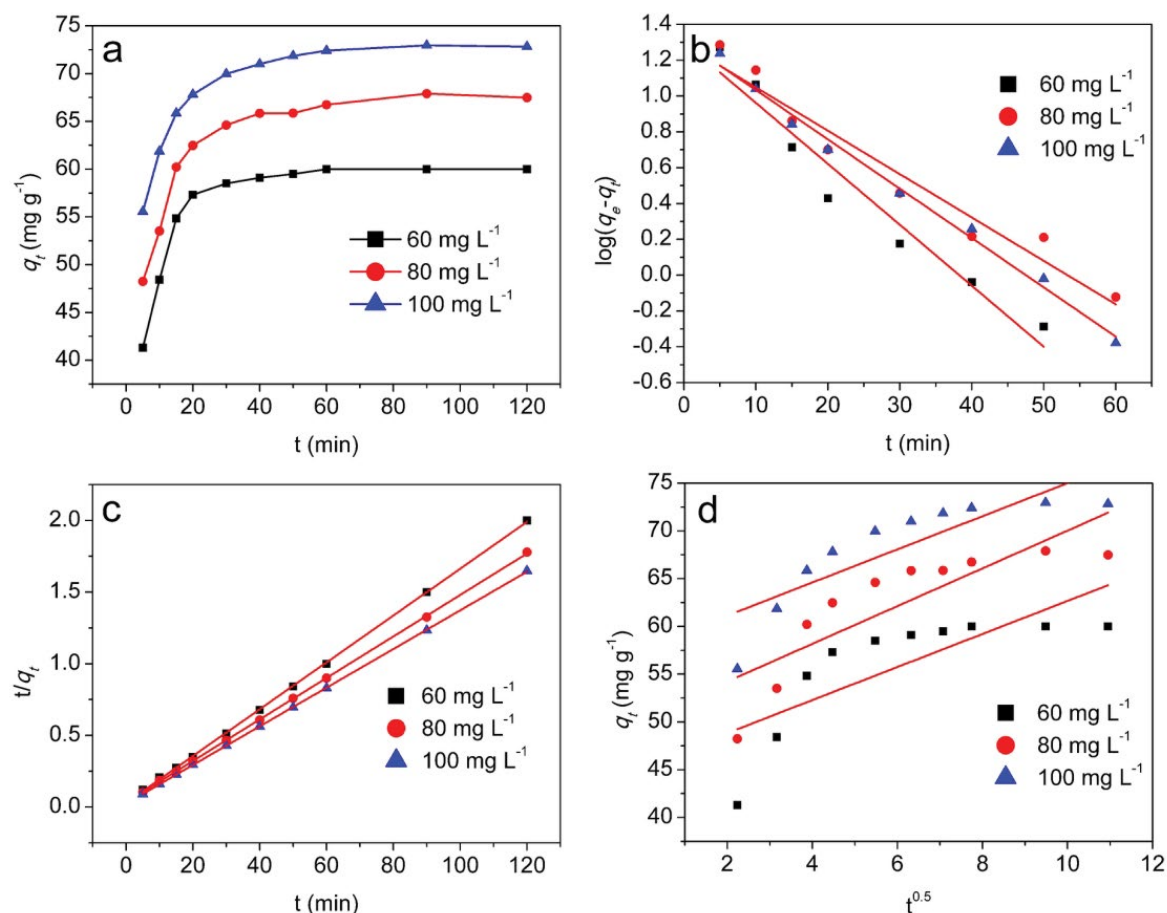
Fig. 3. Experimental plots (a), pseudo-first-order (b), pseudo-second-order (c) and intraparticle diffusion (d) fittings of adsorption kinetics of Ni(II) on NPPFR. Adsorbent dosage = 1 g L^{-1}, pH = 5.0, shaking time = 5–120 min, 303 K.

place on the outer surface of NPPFR and that intraparticle diffusion resistance might be neglected. It is worth noting that almost 100% of the Ni(II) was adsorbed onto the NPPFR when the initial concentration of Ni(II) was 60 mg L^{-1}, which suggested that NPPFR has a strong affinity for Ni(II). This result is very favorable for Ni(II) removal in micro-polluted and low concentrations of Ni(II)-bearing wastewaters.

The kinetic data were further analyzed to determine the rate and mechanism of the reaction and to determine the determination of the rate-controlling step using three well-known kinetic models. The pseudo-first-order [21], pseudo-second-order [22] and intraparticle diffusion [23] equations are represented as Eqs. (4)–(6), respectively.

$$\log\left(q_e - q_t\right) = \log q_e - \frac{k_1 t}{2.303} \tag{4}$$

$$\frac{t}{q_t} = \frac{1}{\left(q_e\right)^2 k_2} + \frac{t}{q_e} \tag{5}$$

$$q_e = k_{id} t^{1/2} + C \tag{6}$$

where q_e and q_t are the amounts of Ni(II) adsorbed (mg g^{-1}) at equilibrium and at time t (min), respectively. k_1 (min^{-1}), k_2 (g mg^{-1} min^{-1}) and k_{id} (mg g^{-1} min$^{-0.5}$) are the pseudo-first-order, pseudo-second-order and intraparticle diffusion rate constant, respectively.

The parameters of the kinetic models are listed in Table S1. The experimental data were better fitted with the pseudo-second-order model. The regression coefficient value ($R^2 > 0.99$) of the pseudo-second-order model was much higher than that of the pseudo-first-order model. Moreover, the values of $q_{e,cal.}$ calculated from the pseudo-second-order model was close to those of $q_{e,exp.}$ determined from tests. These results suggested that the adsorption of Ni(II) closely followed the pseudo-second-order kinetic model in all cases, which indicated that the rate-limiting step was a chemisorption process between Ni(II) and NPPFR.

3.3. Effect of initial concentration and isotherms

The adsorption experiments were carried out at varying initial concentrations of Ni(II) ranging from 20–200 mg L^{-1}. The plot of q_e vs. C_e for the adsorption isotherm of Ni(II) onto NPPFR is shown in Fig. 4a. The uptake of Ni(II) increased sharply as the initial metal concentration increased up to
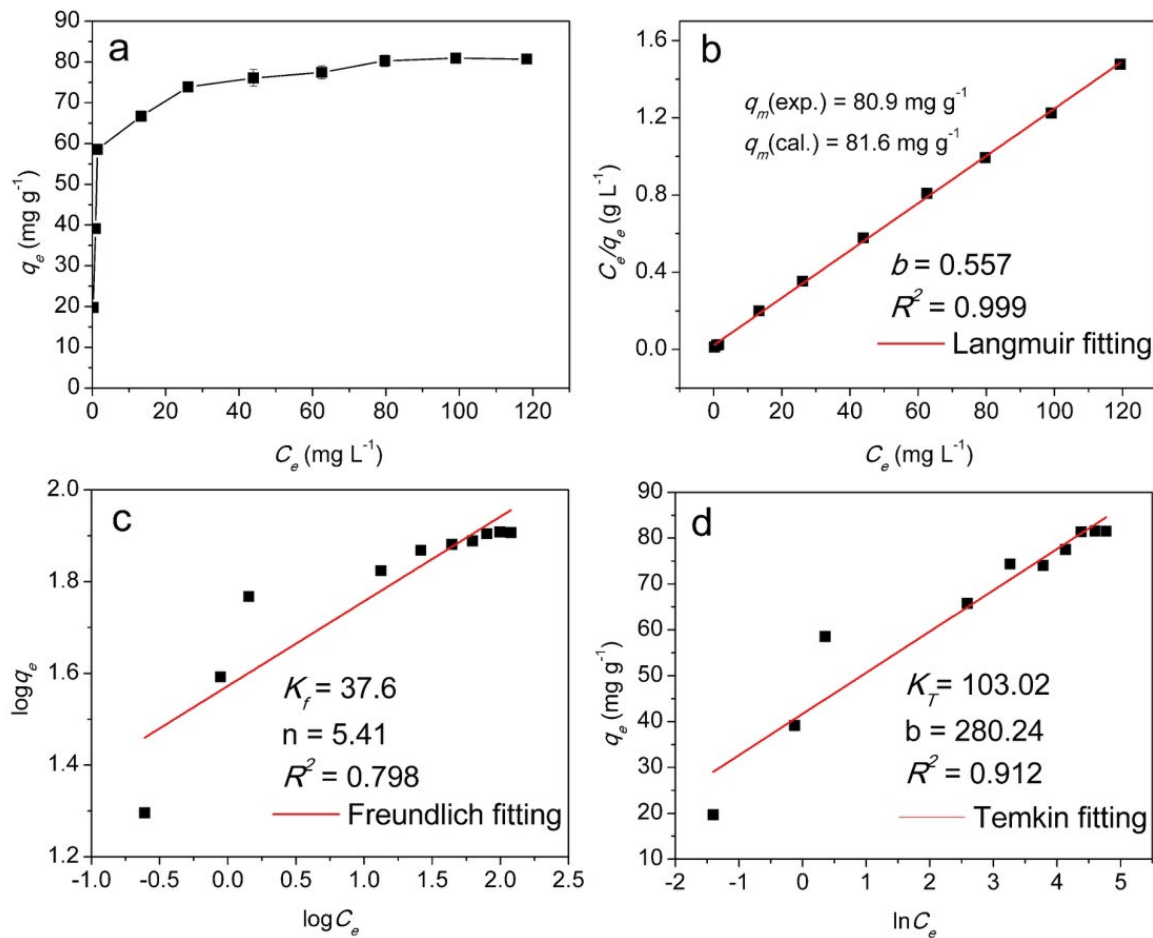
Fig. 4. Adsorption isotherm of Ni(II) onto NPPFR (a), Langmuir fitting (b), Freundlich fitting (c) and Temkin fitting (d).

60 mg L^{-1}, and then slightly increased, followed by a plateau at high concentrations of Ni(II). The isothermal data were applied to the Langmuir, Freundlich and Temkin models.

The Langmuir isotherm, a monolayer adsorption model, assumes that there is a limited capacity of the solid adsorbent and that all the adsorption sites are identical [24]. The Freundlich adsorption isotherm, an empirical model, implies heterogeneous adsorption sites and is highly suitable for modeling adsorption at low solution concentrations [25]. Temkin and Pyzhev considered the effects of some indirect adsorbate/adsorbate interactions on adsorption isotherms and their model explains that the heat of adsorption of all the molecules in the layer will decrease linearly with coverage [26].

The linear forms of the Langmuir, Freundlich and Temkin isotherms can be expressed as Eqs. (7)–(9), respectively.

$$\frac{C_e}{q_e} = \frac{C_e}{q_m} + \frac{1}{bq_m} \tag{7}$$

where C_e is the equilibrium concentration of Ni(II) remained in the solution after adsorption, q_e is the equilibrium amount adsorbed (mg g^{-1}), q_m is the monolayer capacity of Ni(II)

adsorbed on the adsorbent (mg g^{-1}) and b is the Langmuir constant related to the energy (L mg^{-1}).

$$\log q_e = \log K_f + \frac{1}{n}\log C_e \tag{8}$$

where K_f and n are the Freundlich isotherm constants indicating the adsorption capacity and intensity, respectively.

$$q_e = \frac{RT}{b}\ln K_T + \frac{RT}{b}\ln C_e \tag{9}$$

where K_T and b is the Temkin isotherm constants (L mol^{-1}).

It can be seen from Fig. 4b–d that the Langmuir mode fitted the experimental data well according to the high regression coefficient value ($R^2 > 0.99$), which illustrated that the biosorption proceeded via monolayer sorption on the surface of the adsorbent NPPFR. According to the Langmuir equation, the maximum monolayer adsorption capacity was calculated to be 81.6 mg g^{-1}, which is close to the experimental data. The isotherm constants can predict whether an adsorption system is favorable or not. The essential features of the Langmuir isotherm can be expressed in

terms of a dimensionless constant, the separation factor (R_L), which is defined as:

$$R_L = \frac{1}{1 + K_L C_i} \tag{10}$$

where K_L is the Langmuir constant (L mg^{-1}) and C_i is the highest initial metal concentration (mg L^{-1}). The value of R_L indicates whether the isotherm is unfavourable ($R_L > 1$), linear ($R_L = 1$), favourable ($0 < R_L < 1$) or irreversible ($R_L = 0$) [27]. The value of R_L was 0.9913, which indicates a favorable adsorption process.

The favourability of adsorption can also be revealed by the n value of the Freundlich fitting, the value of n ($n = 5.41$) is in the range of 2–10, indicating that the adsorption between NPPFR and Ni(II) is favorable and proceeds easily. The correlation coefficients of the Temkin model ($R^2 = 0.912$) were much better than those of the Freundlich model, so the Temkin model could also describe the adsorption process.

A comparative study of the adsorption capacities of different bio-adsorbents for the removal of Ni(II) is listed in Table 1. NPPFR has a much higher adsorption capacity in the range of low initial concentrations of Ni(II) than some other adsorbents reported in the literature.

3.4. Effect of temperature and thermodynamic studies

To determine the thermodynamic parameters, batch experiments were carried out at different temperatures in the range of 293–323 K for Ni(II) adsorption. Fig. 5 shows that increasing the temperature slightly decreases the adsorption capacity for Ni(II), which indicates that the adsorption is an exothermic process. The thermodynamic parameters, such as the free Gibbs energy ($\Delta G°$), enthalpy ($\Delta H°$), and entropy ($\Delta S°$) were computed using the following equations:

$$K_c = \frac{C_{ads}}{C_e} \tag{11}$$

$$\ln K_c = \frac{-\Delta H°}{RT} + \frac{\Delta S°}{R} \tag{12}$$
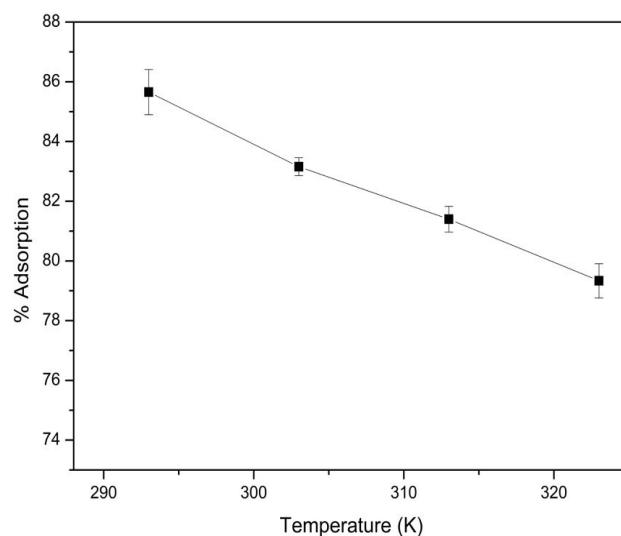
Fig. 5. Effect of temperature on Ni(II) adsorption.

$$\Delta G° = -RT \ln K_c \tag{13}$$

where K_c is the equilibrium constant, C_{ads} is the amount of Ni(II) adsorbed by NPPFR (mg L^{-1}) at equilibrium, C_e is the amount of Ni(II) remaining in the solution (mg L^{-1}) at equilibrium, R (8.314 J mol^{-1} K^{-1}) is the universal gas constant, and T is the solution temperature (K) in Kelvin [28].

The values of $\Delta G°$, $\Delta H°$, and $\Delta S°$ are shown in Table 2. The negative $\Delta G°$ values increased with temperature, indicating the spontaneity of the adsorption process of Ni(II) onto NPPFR. The negative $\Delta H°$ indicated the exothermic nature of the adsorption process and the negative $\Delta S°$ signified a decrease in the randomness at the solid-solution interface of Ni(II) and the NPPFR surface. In addition, based on the $\Delta S°$ value, there are associative and dissociative mechanisms, and when $\Delta S° < -10$ J mol^{-1} k^{-1}, the associative mechanism becomes a dominant [29]. In this work, the value of $\Delta S°$ of -17 J mol^{-1} k^{-1} for Ni(II) indicated that the adsorption process followed the associative mechanism.

Table 1
Comparison of adsorption capacity of various bioadsorbents for the removal of Ni(II) from aqueous solutions

Adsorbents	Q_{max} (mg g^{-1})	Solution pH	Range of initial concentrations (mg L^{-1})	Reference
Cashew nut shell	18.9	pH 5	10–50	[1]
Modified orange peel	162.6	pH 5.5	0–600	[4]
Sugarcane bagasse pith	73.6	pH 6.5	50–1,000	[7]
Moringa oleifera bark	45.0	pH 6	20–200	[8]
Mercerized pine bark	23.7	pH 5	0–100	[9]
Lithothamnium calcareum algae	54.9	pH 5	5–500	[10]
Histidine modified chitosan beads	55.6	pH 5	25–1,000	[11]
Chitosan immobilized on bentonite	15.8	pH 4	50–500	[12]
Grafted hydrazinyl amine magnetite-chitosan	254.2	pH 5	5–300	[13]
NaOH treated persimmon powder-formaldehyde resin (NPPFR)	81.6	pH 5	20–200	This work

Table 2
Thermodynamic parameters for the adsorption of Ni(II) on NPPFR (C_i = 80 mg L^{-1})

Temp. (K)	K_c	$\Delta G°$ (kJ mol^{-1})	$\Delta H°$ (kJ mol^{-1})	$\Delta S°$ (kJ mol^{-1} K^{-1})
293	5.50	–4.15	–9.39	–0.017
303	4.94	–4.02		
313	4.38	–3.84		
323	3.84	–3.61		

3.5. Desorption and regeneration studies

The reusability of spent adsorbent NPPFR is important for technical application. Desorption studies of Ni(II) from NPPFR were carried out by using HNO$_3$ solutions. After one sorption-desorption cycle, NPPFR was regenerated with 0.1 mol L^{-1} NaOH, rinsed with deionized water, and then reused and desorbed again. These cycles were repeated four times. As shown in Table 3, the desorption efficiency was 94.0%–95.2% at various concentrations of HNO$_3$. Since little improvement was made when the HNO$_3$ concentration was increased, 0.1 mol L^{-1} HNO$_3$ was chosen as the optimal desorption reagent. The reusability of NPPFR for four repeated adsorption-elution cycles is also shown in Table 3. The amount of Ni(II) (q_e) adsorbed onto the adsorbent and desorption efficiency almost remained almost the same, which indicated that NPPFR can be repeatedly used in the biosorption process of Ni(II) removal.

3.6. Effect of coexisting metal ions

It is well known that the presence of one heavy metal may hinder the adsorption of other heavy metals [2]. Thus, the investigation of the effects of coexisting metal ions is useful at the industrial scale. The adsorption of Ni(II) in the presence of coexisting cations (Pb(II), Zn(II), Mn(II), Mg(II), K(I) and Na(I)) was evaluated in binary metal ion systems containing 80 mg L^{-1} metal ions. Fig. 6a shows that the adsorption percentage of Ni(II) in a single-metal solution was higher than that in binary metal ion systems of Pb(II), Zn(II), Mn(II) and Mg(II). This can be attributed to the competition between heavy metal ions, and the effects of competing cations on Ni(II) adsorption decreased in the orders of Pb(II) >> Zn(II) > Mn(II) > Mg(II). Similar phenomena have been observed for the competitive adsorption of Cu(II), Pb(II) and Ni(II) on chitosan immobilized on bentonite [12].

Table 3
Desorption and regeneration of NPPFR in adsorption-elution cycles

Cycles (C_i = 80 mg L^{-1})	q_e (mg g^{-1})	% Desorption	Desorption efficiency (%) of Ni(II) using HNO$_3$ (mol L^{-1})				
			0.1	0.2	0.3	0.4	0.5
1	67.7	94.1	94.1	94.0	94.6	95.2	95.1
2	66.6	93.2					
3	67.2	92.9					
4	67.4	93.4					
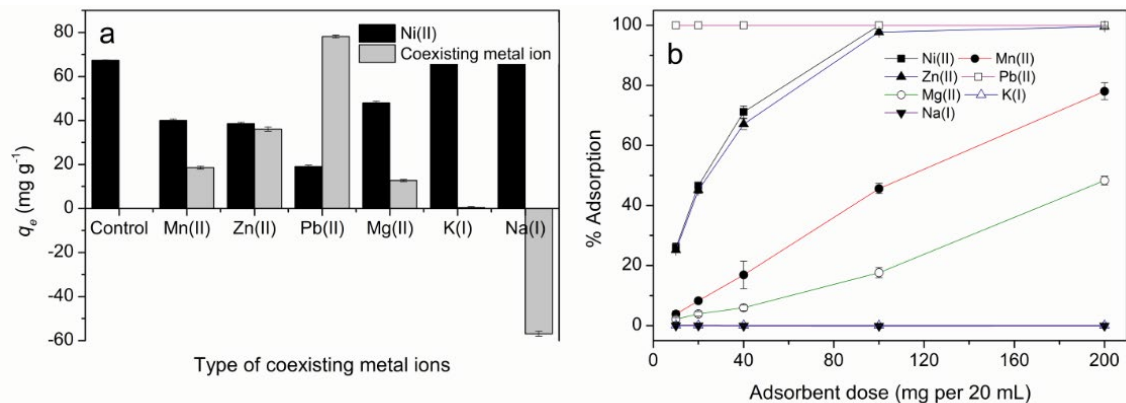
Fig. 3. Effects of coexisting metal ions on Ni(II) adsorption (a), initial concentration of metal ions = 80 mg L^{-1}) and effect of NPPFR dose on the adsorption of Ni(II) from actual wastewater (b), containing 25.2, 4.6, 15.5, 34.2, 9.3, 950.6, 8.3 mg L^{-1} of Ni(II), Pb(II), Zn(II), Mn(II), Mg(II), Na(I) and K(I), respectively, pH = 5.24).

The presence of Na(I) and K(I) had no significant effects on the adsorption of Ni(II). However, the concentration of Na(I) increased due to the release of Na(I) into the solution from the adsorbent NPPFR surface in the Ni(II)-Na(I) binary metal ion system, which supports that the adsorption occurs via ionic exchange between Na(I) on NPPFR and Ni(II).

3.7. Applicability to industrial wastewaters

The applicability of the investigated adsorbent material, NPPFR, was demonstrated by treating actual industrial wastewaters containing Ni(II). Samples of Ni(II)-bearing industrial wastewaters (containing 25.2, 4.6, 15.5, 34.2, 9.3, 950.6, and 8.3 mg L^{-1} of Ni(II), Pb(II), Zn(II), Mn(II), Mg(II), Na(I) and K(I), respectively) were kindly provided by Jingmen GEM New Materials Co. Ltd., China. The influence of adsorbent dose on Ni(II) removal in the presence of various ions by NPPFR from industrial wastewaters is shown in Fig. 6b. According to Fig. 6b, Na(I) and K(I) ions were not adsorbed onto the adsorbent NPPFR. The percent adsorption of the metals Ni(II), Zn(II), Mn(II), and Mg(II) increased with increasing adsorbent dose. This can be attributed to the greater availability of adsorption sites or surface area at higher doses of the adsorbent. The complete removal of Ni(II) from 20 mL of simulated and industrial wastewater samples was achieved with an adsorbent dose of 100 mg. The results showed that a minimum adsorbent dose of 100 mg in 20 mL of wastewater (5 g L^{-1}) is sufficient for the removal of Ni(II) from industrial wastewaters.

Continuous adsorption and elution experiments were carried out on a packed column bed with 500 mg NPPFR. From the breakthrough curve shown in Fig. 7a, the breakthrough of K(I) and Na(I) occurred immediately after the start of flow, and then the breakthrough of other metal ions Mg(II), Mn(II), Ni(II), Zn(II) and Pb(II) started at 90, 220, 460, 740, and 1,020-bed volumes (B.V.), respectively.

It is noteworthy that the C_e/C_i values of Mg(II), Mn(II), Ni(II), and Zn(II) were greater than 1.0, which is not typical behavior of a breakthrough curve. As mentioned above, ion competition existed in the adsorption process, and it is reasonable to propose that ions of Mg(II), Mn(II), Ni(II), and

Zn(II) adsorbed onto the surface of the NPPFR were replaced by stronger-affinity ions such as Pb(II). However, the existence of competition and replacement between metal ions does not affect the application of the adsorbent for Ni(II) removal from aqueous solutions. NPPFR is an effective and low-cost adsorbent, where 500 mg of adsorbent can deal with treat a large volume of wastewater as high as much as 414 mL (420 B.V.).

Once the column adsorption reached adsorption saturation, the loaded metal ions were eluted with 0.1 mol L^{-1} HNO_3. The elution profiles of metal ions are shown in Fig. 7b, which shows that all the metal ions were eluted with preconcentration factors of 13.7 for Pb(II), 12.0 for Mg(II), 12.0 for Mg(II), 3.09 for Zn(II), 1.42 for Ni(II), and 0.78 for Mn(II). The low preconcentration factors of Zn(II), Ni(II), and Mn(II) also indicated the competition and replacement of metal ions in the multiple metal ion systems.

3.8. Characterization

FT-IR spectra of NPPFR before and after adsorption of Ni(II) are shown in Fig. S1. The broadband at 3,394 cm^{-1} is due to phenolic O–H stretching vibration. The weak band at 1,712 cm^{-1} and the sharp band at 1,612 cm^{-1} are attributed to the C=O stretching vibrations of ester and ketone groups, and the band at 1,446 cm^{-1} is due to ring C–C stretching vibrations. The peaks observed at 1,380; 1,213; and 1,112 cm^{-1} are assigned to O–H bending vibrations, C=C–O stretching, and C–O stretching vibrations, respectively. After adsorption of Ni(II), the O–H vibrations at 3,394 cm^{-1} and 1,380 had shifted to 3,389 and 1,389 cm^{-1}, respectively. These shifts may be caused by the changes in counter ions associated with hydroxyl anions via ion exchange.

Before adsorption, the surface of the NPPFR particles was rough and irregular, as shown in Fig. 8a and the characteristic peaks of C, O and Na were found in the EDS spectrum shown in Fig. 8b, which indicated that there was a large amount of Na(I) on the surface of the NPPFR adsorbent and confirmed that the NaOH modification was successful. In addition, the small specific surface area assayed by the N_2 adsorption/desorption test shows that the functional groups
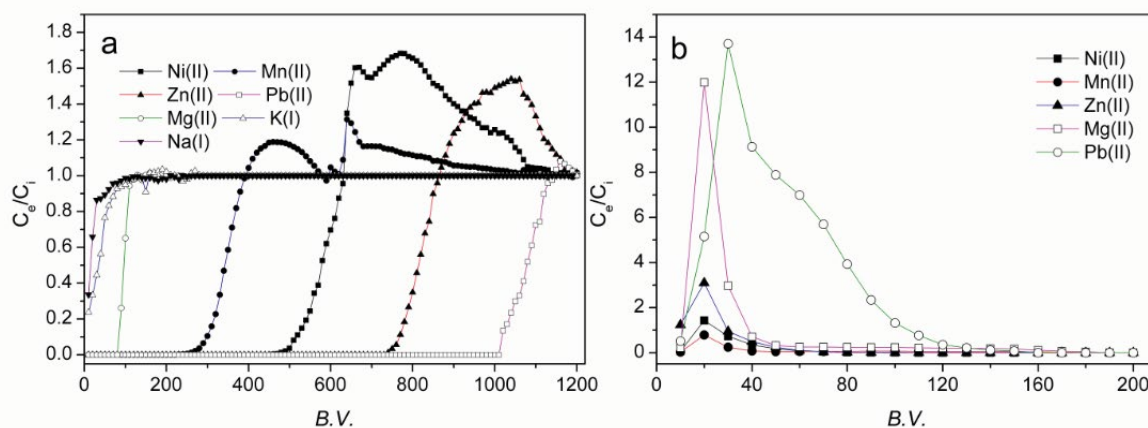
Fig. 7. Breakthrough (a) and elution (b) profiles of actual wastewaters with a column packed with 500 mg NPPFR. Flow rate = 9 mL h^{-1}, room temperature.
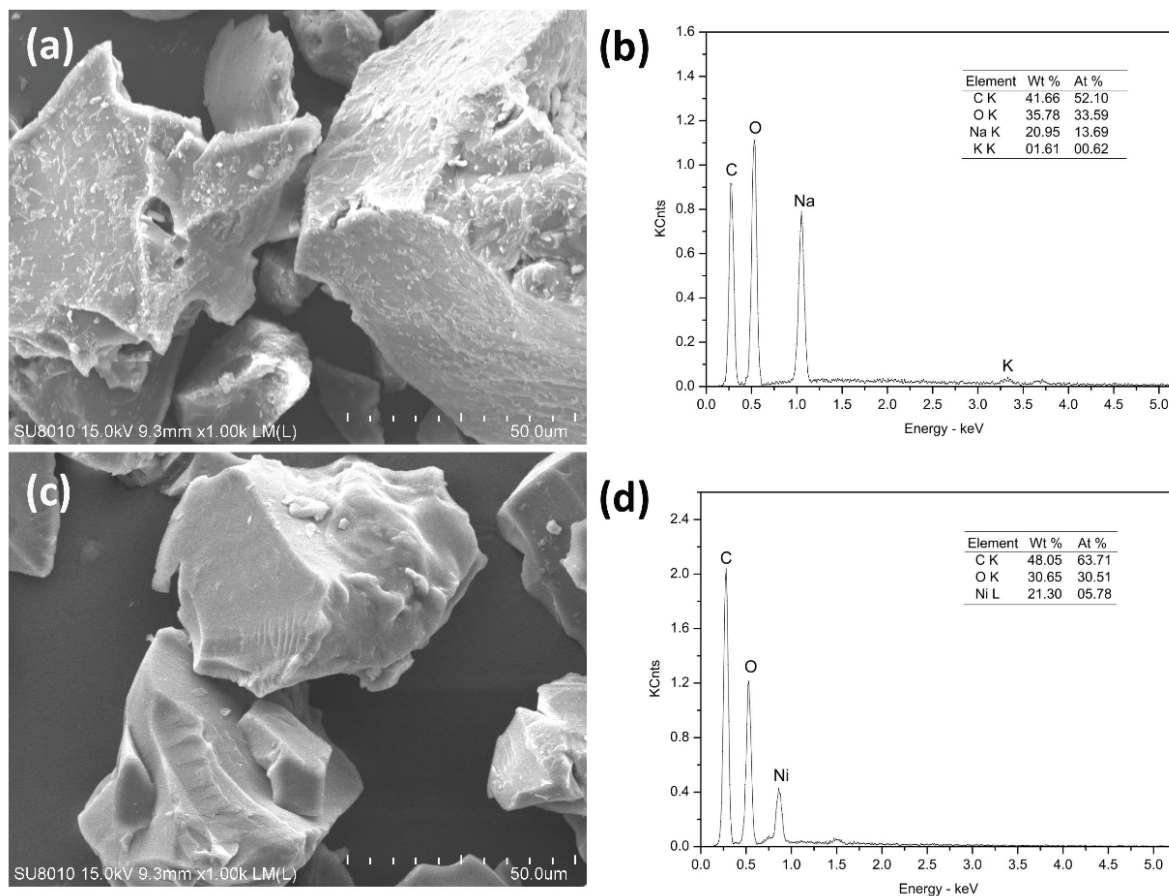
Fig. 8. SEM-EDS of NPPFR (a,b) before adsorption, (c,d) after adsorption of Ni(II).

in the resin are more efficient than the surface area in the sorption process. After adsorption of Ni(II), Fig. 8c shows that the surface of the adsorbent was covered with a thin layer and became smooth. This result indicated that the adsorbed Ni(II) might be bonded on the surface of NPPFR which was consistent with the best fitting of the Langmuir monolayer adsorption model. In the EDS spectrum shown in Fig. 8d, there are characteristic peaks of C, O, and Ni without Na characteristic peaks. These results indicate that Ni(II) was not only adsorbed on the surface of NPPFR but also exchanged with Na(I).

3.9. Adsorption mechanism of Ni(II) onto NPPFR

Previous studies have shown that tannins are rich in phenolic hydroxyl groups, which can form coordinated covalent bonds with a metal cation such as Pb(II) and Cu(II) [30,31]. In this experiment, however, PPFR showed little affinity towards Ni(II) in aqueous solutions, and the NaOH modified adsorbent NPPFR showed a significant increase in the adsorption capacity of Ni(II). Therefore, the proposed adsorption mechanism shown in Fig. S2 illustrates that some of the phenolic hydroxyl groups of PPFR reacted with NaOH in the alkali treatment, leading to hydrogen replacement by sodium in the adsorbent NPPFR, and the binding site of NPPFR contains a large amount of Na(I), which has a strong

interaction with Ni(II). Therefore, the adsorption mechanism of NPPFR on Ni(II) can be summarized as follows: (1) electrostatic attraction between negatively charged active sites on NPPFR and Ni(II); and (2) ionic exchange between Na(I) and Ni(II). Additionally, the results of coexisting ions and adsorption-desorption experiments show the competition and replacement of metal ions in multiple metal ion systems.

4. Conclusions

The removal of Ni(II) from aqueous solutions using persimmon residual-based bio-sorbents was evaluated. Among the 4 types of persimmon tannin adsorbents, NPPFR showed a significantly enhanced capacity for the adsorption of Ni(II). The adsorption of Ni(II) was dependent on the initial pH of the solution and occurred rapidly within 60 min, and the maximum adsorption capacity by NPPFR was evaluated as 81.6 mg g^{-1} at pH 5.0. The pseudo-second-order kinetics and the Langmuir isotherm models precisely fit the experimental data. The removal of Ni(II) from actual industrial wastewaters in both batch and column experiments was proven to be effective, and the loaded metals could be easily desorbed by 0.1 mol L^{-1} HNO$_3$. The adsorption mechanism was proposed to be electrostatic attraction and ion exchange. This work illustrates that NPPFR can be utilized as a low-cost and effective alternative for the elimination of Ni(II) from

aqueous solutions due to its high sorption capacity, reusability and abundance.

Acknowledgments

References

[1] P.S. Kumar, S. Ramalingam, S.D. Kirupha, A. Murugesan, T. Vidhyadevi, S. Sivanesan, Adsorption behavior of nickel (II) onto cashew nut shell: equilibrium, thermodynamics, kinetics, mechanism and process design, Chem. Eng. J., 167 (2011) 122–131.

[2] T.A.H. Nguyen, H.H. Ngo, W.S. Guo, J. Zhang, S. Liang, Q.Y. Yue, Q. Li, T.V. Nguyen, Applicability of agricultural waste and by-products for adsorptive removal of heavy metals from wastewater, Bioresour. Technol., 148 (2013) 574–585.

[3] B. Liu, X. Chen, H. Zheng, Y. Wang, Y. Sun, C. Zhao, S. Zhang, Rapid and efficient removal of heavy metal and cationic dye by carboxylate-rich magnetic chitosan flocculants: role of ionic groups, Carbohydr. Polym., 181 (2018) 327–336.

[4] N. Feng, X. Guo, S. Liang, Y. Zhu, J. Liu, Biosorption of heavy metals from aqueous solutions by chemically modified orange peel, J. Hazard. Mater., 185 (2011) 49–54.

[5] M. Fomina, G.M. Gadd, Biosorption: current perspectives on concept, definition and application, Bioresour. Technol., 160 (2014) 3–14.

[6] M.N. Zafar, I. Aslam, R. Nadeem, S. Munir, U.A. Rana, S.U.D. Khan, Characterization of chemically modified biosorbents from rice bran for biosorption of Ni (II), J. Taiwan Inst. Chem. Eng., 46 (2015) 82–88.

[7] K.A. Krishnan, K.G. Sreejalekshmi, R.S. Baiju, Nickel (II) adsorption onto biomass based activated carbon obtained from sugarcane bagasse pith, Bioresour. Technol., 102 (2011) 10239–10247.

[8] D.H.K. Reddy, D.K.V. Ramana, K. Seshaiah, A.V.R Reddy, Biosorption of Ni (II) from aqueous phase by *Moringa oleifera* bark, a low cost biosorbent, Desalination, 268 (2011) 150–157.

[9] A.L. Arim, G. Guzzo, M.J. Quina, L.M. Gando-Ferreira, Single and binary sorption of Cr(III) and Ni(II) onto modified pine bark, Environ. Sci. Pollut., 25 (2018) 28039–28049.

[10] D.M. Veneu, L. Yokoyama, O.G.C. Cunha, C.L. Schneider, M.B. de Mello Monte, Nickel sorption using bioclastic granules as a sorbent material: equilibrium, kinetic and characterization studies, J. Mater. Res. Technol., 8 (2019) 840–852.

[11] A. Eser, V.N. Tirtom, T. Aydemir, S. Becerik, A. Dinçer, Removal of nickel (II) ions by histidine modified chitosan beads, Chem. Eng. J., 210 (2012) 590–596.

[12] C.M. Futalan, C.C. Kan, M.L. Dalida, K.J. Hsien, C. Pascua, M.W. Wan, Comparative and competitive adsorption of copper, lead, and nickel using chitosan immobilized on bentonite, Carbohydr. Polym., 83 (2011) 528–536.

[13] M.F. Hamza, Y. Wei, H.I. Mira, A.H. Adel, E. Guibal, Synthesis and adsorption characteristics of grafted hydrazinyl amine magnetite-chitosan for Ni(II) and Pb(II) recovery, Chem. Eng. J., 362 (2019) 310–324.

[14] A. Nakajima, Y. Baba, Mechanism of hexavalent chromium adsorption by persimmon tannin gel, Water Res., 38 (2004) 2859–2864.

[15] M. Gurung, B.B. Adhikari, S. Alam, H. Kawakita, K. Ohto, K. Inoue, Persimmon tannin-based new sorption material for resource recycling and recovery of precious metals, Chem. Eng. J., 228 (2013) 405–414.

[16] Q. Yi, R. Fan, F. Xie, Q. Zhang, Z. Luo, Recovery of Palladium(II) from nitric acid medium using a natural resin prepared from persimmon dropped fruits residues, J. Taiwan Inst. Chem. Eng., 61 (2016) 299–305.

[17] A. Szczurek, G. Amaral-Labat, V. Fierro, A. Pizzi, A. Celzard, Chemical activation of tannin-based hydrogels by soaking in KOH and NaOH solutions, Microporous Mesoporous Mater., 196 (2014) 8–17.

[18] F. Xie, Z. Fan, Q. Zhang, Z. Luo, Selective adsorption of Au³⁺ from aqueous solutions using persimmon powder–formaldehyde resin, J. Appl. Polym. Sci., 130 (2013) 3937–3946.

[19] M. Gurung, B.B. Adhikari, H. Kawakita, K. Ohto, K. Inoue, S. Alam, Recovery of gold and silver from spent mobile phones by means of acidothiourea leaching followed by adsorption using biosorbent prepared from persimmon tannin, Hydrometallurgy, 133 (2013) 84–93.

[20] K. Vijayaraghavan, Y.S. Yun, Bacterial biosorbents and biosorption, Biotechnol. Adv., 26 (2008) 266–291.

[21] S.C. Tsai, T.H. Wang, Y.Y. Wei, W.C. Yeh, Y.L. Jan, S.P. Teng, Kinetics of Cs adsorption/desorption on granite by a pseudo-first-order reaction model, J. Radioanal. Nucl. Chem., 275 (2008) 555–562.

[22] Y.S. Ho, G. McKay, Pseudo-second-order model for sorption processes, Process Biochem., 34 (1999) 451–465.

[23] M.S. Chiou, H.Y. Li, Adsorption behavior of reactive dye in aqueous solution on chemical cross-linked chitosan beads, Chemosphere, 50 (2003) 1095–1105.

[24] I. Langmuir, The constitution and fundamental properties of solids and liquids, Part I. Solids, J. Am. Chem. Soc., 38 (1916) 2221–2295.

[25] H. Freundlich, Over the adsorption in solution, J. Phys. Chem., 57 (1906) 385–470.

[26] M.J. Temkin, V. Pyzhev, Kinetics of ammonia synthesis on promoted iron catalysts, Acta Phys. Chim. URSS, 12 (1940) 217–222.

[27] M.M. Tehrani, S. Abbasizadeh, A. Alamdari, S.E. Mousavi, Prediction of simultaneous sorption of copper(II), cobalt(II) and zinc(II) contaminants from water systems by a novel multi-functionalized zirconia nanofiber, Desal. Wat. Treat., 62 (2017) 403–417.

[28] A. Sari, M. Tuzen, D. Citak, M. Soylak, Equilibrium, kinetic and thermodynamic studies of adsorption of Pb(II) from aqueous solution onto Turkish kaolinite clay, J. Hazard. Mater., 149 (2007) 283–291.

[29] M. Bozorgi, S. Abbasizadeh, F. Samani, S.E. Mousavi, Performance of synthesized cast and electrospun PVA/chitosan/ZnO-NH₂ nano-adsorbents in single and simultaneous adsorption of cadmium and nickel ions from wastewater, Environ. Sci. Pollut. Res., 25 (2018) 17457–17472.

[30] M. Yurtsever, İ.A. Şengil, Biosorption of Pb(II) ions by modified quebracho tannin resin, J. Hazard. Mater., 163 (2009) 58–64.

[31] Q. Xu, Y. Wang, L. Jin, Y. Wang, M. Qin, Adsorption of Cu(II), Pb(II) and Cr(VI) from aqueous solutions using black wattle tannin-immobilized nanocellulose, J. Hazard. Mater., 339 (2017) 91–99.

Supplementary information

Table S1
Kinetic parameters for the adsorption of Ni(II) onto NPPFR

C_i (mg L^{-1})	$q_{e,\text{exp.}}$ (mg g^{-1})	Pseudo-first-order		Pseudo-second-order			Intraparticle diffusion		
		k_1 (min^{-1})	R^2	$q_{e,\text{cal.}}$ (mg g^{-1})	k_2 (g mg^{-1} min^{-1})	R^2	k_{id} (mg g^{-1} min$^{-0.5}$)	R^2	C
60	60.0	0.0790	0.943	62.7	0.00662	0.999	1.730	0.546	45.38
80	67.6	0.0310	0.993	68.4	0.00246	0.999	1.974	0.670	50.28
100	74.2	0.0389	0.946	74.9	0.00649	1.000	1.734	0.690	57.67
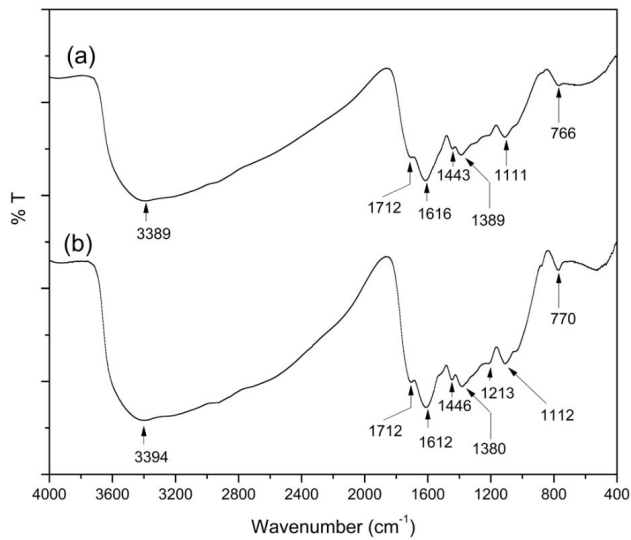
Fig. S1. FT-IR spectra of NPPFR (a) before adsorption and (b) after adsorption of Ni(II).
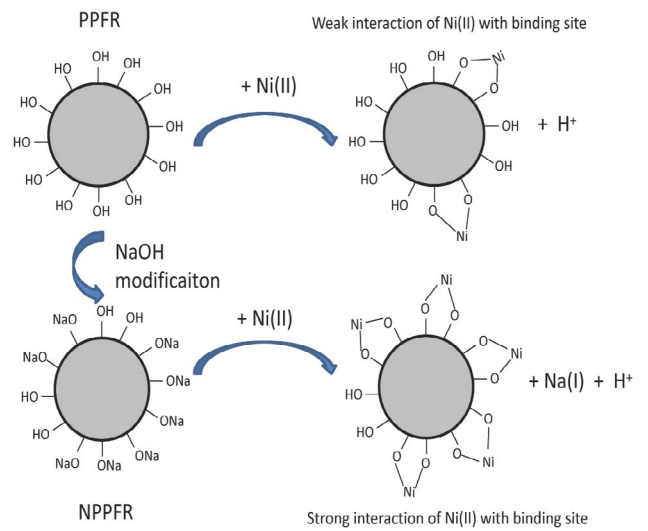
Fig. S2. Proposed adsorption mechanism between the adsorbents and Ni(II) ions.